COMPOSITIONAL AND STRUCTURAL CHARACTERISTICS OF SCHRÖDINGER'S BASIN VOLCANISM. G. Y Kramer[1], D. A. Kring[1], P. J. McGovern[1], A. L. Nahm[2], T. Ohman[1,3]; [1] Lunar & Planetary Science Institute, Houston, TX, [2] University of Idaho, Moscow, ID, [3]Arctic Planetary Science Institute, Rovaniemi, Finland.

Introduction

Schrödinger Basin is 315 km in diameter and is located at 75°S, 132.5°E, which places it on the western rim of the oldest and largest lunar basin, South Pole-Aitken (SPA). More precisely, Schrödinger is nestled between the outer edge of SPA's transient crater and the final basin rim [1, 2]. Schrödinger is one of the youngest lunar basins, only marginally older than Orientale [3, 4]. It has been targeted as an ideal location for a future landing site [5] since it is thought to have tapped deep crustal lithologies associated with the SPA basin-forming event [6], contain ejected lithologies from the Orientale basin-forming event, and has later mare and pyroclastic eruptions on its floor.

Basin-related pyroclastic volcanism may represent the last phase of volcanic activity in some regions on the Moon. Remote sensing studies have shown that volcanic glasses are fairly common and often found along the perimeter of mare-filled basins [7]. Modeling of the stresses related to the basin-forming process [8,9] show that basin margins provide the ideal conduit for low-volume lunar pyroclastic volcanism (as compared to the high output of mare volcanism).

Schrödinger Basin provides an interesting location to study the phenomenon. 1) Its proximity to SPA may have encouraged late-stage volcanism by providing closer access to the deep crust and/or mantle. 2) The basin is not filled with mare basalt; instead the floor is largely composed of a compositionally uniform impact breccia [6]. The exceptions are two distinct and spatially isolated volcanic units, both confined within the central peak ring (Fig. 1a). One is a thin mare deposit to the north, and to the south is an 8.6 km-long pyroclastic vent. 3) The basin floor has a complex set of fractures that postdate formation of the basin; some of which are associated with the later onset of volcanism [6,10,11,12,13,14].

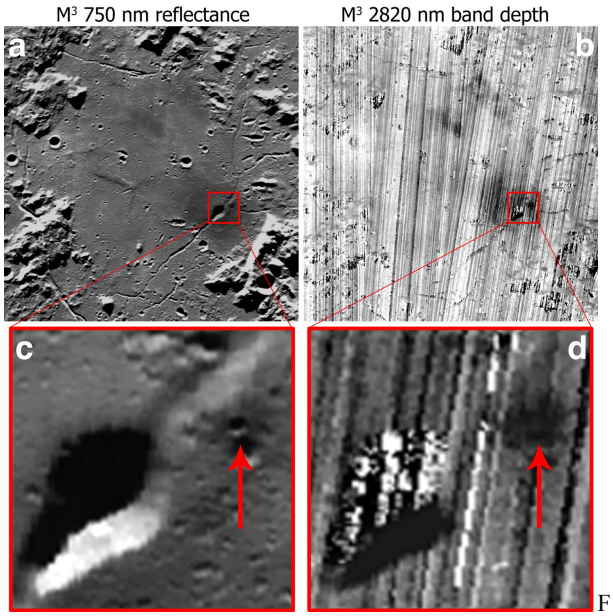

Fig. 1: **(a)** M³ 750 nm albedo image of Schrödinger's peak ring and interior. **(b)** Map of same region as **a**, showing relative OH abundance based on the depth of the 2820 nm absorption. Dark areas have lower OH. **(c)** Close-up of pyroclastic vent (box in **a**). **(d)** Relative OH abundance map of pyroclastic vent (box in **b**). Arrows point to a fresh crater in pyroclastic deposits (see text).

We have been studying Schrödinger through a coordinated effort utilizing our different expertise in spectroscopy, petrology, photogeology, geophysics, structural geology, and impact cratering mechanics using data sets including Lunar Reconnaissance Orbiter's (LRO) Wide Angle Camera (WAC) and Narrow Angle Camera (NAC) images, topography from LRO's Orbiting Laser Altimeter (LOLA), and spectral data from the Chandrayaan-1's Moon Mineralogy Mapper (M^3) to fully characterize the geology and history of Schrödinger Basin [6,10,11].

Schrödinger's Fractures

Most of Schrödinger's fractures are associated with the formation of the basin [6,11]. The exception is a system of fractures on the basin floor inside the peak ring that suggests a relationship to Schrödinger's later volcanic activity [10,11,13]. We are working to understand whether this system of fractures is associated with the formation of the basin, if the volcanic event simply utilized an already existing conduit, or whether an expanding magma chamber once resided in this location, uplifted the basin floor, and formed these inter-peak ring fractures [14]. Whether or not the fractures existed there prior to volcanic activity, it is apparent that the magma reservoir emptied via a propagating dike and sill complex, and eventually surfaced at the location of the pyroclastic vent. Did the dramatically altered stress states that resulted from the formation of the basin provide pathways ideally suited for magma ascent?

Schrödinger's Volcanic Units

Schrödinger has two volcanic units, both of which occur inside of its peak ring [6,15] (Fig. 2). The mare basalt unit is located interior to the NNE portion of the inner peak ring. It is identified morphologically by its smooth, dark surface, and distinct flow morphology. It is also distinguished from the surrounding impact breccia floor material by its lower crater population density and characteristic mare basalt spectrum. The unit cannot be thicker than 50 m because craters as small as 450 m diameter have spectra that resemble the adjacent impact

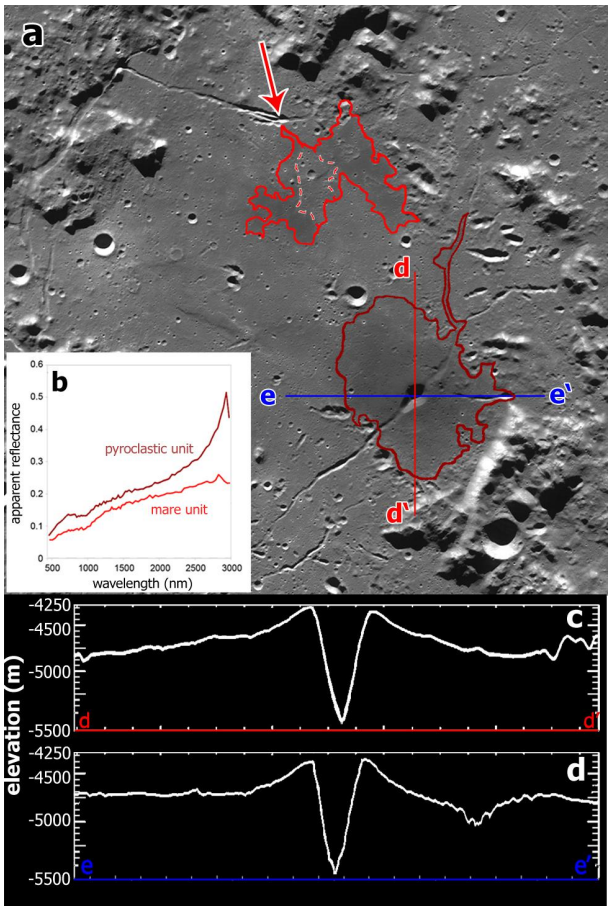

Fig. 2: **(a)** Map of Schrödinger's volcanic units; mare unit in the north, pyroclastic unit in the south. Extent of map the same as in Fig. 1a. **(b)** M^3 spectra of Schrödinger's volcanic units using the same colors to match the spectra to the unit. Outline color in **a**. Transects across pyroclastic vent show the locations of the topographic profiles **(c)** north-south and **(d)** east-west. Profiles have 10 times vertical exaggeration.

breccia floor material, indicating they have penetrated the mare. The source vent is the eastern end of a graben located in the northern portion of the inner peak ring floor material (Fig. 2).

Schrödinger's pyroclastic volcanism occurred to the SSE inside the peak ring. An apron of volcanic glass covers an area of ~1150 km^2 around the vent (Fig. 1a). The pyroclastic material exhibits a characteristically glassy spectrum - low albedo, broad and weak mafic absorption features, and a steep, linear continuum slope (Fig. 2b). The structure extending NE from the vent is the only linear depression that has spectral evidence of the volcanic material. Whether this structure is an exposed dike, a fracture later filled with volcanic material, or carved by flowing volcanic material is still under investigation. Like the mare unit, the pyroclastic unit has a lowest crater density than the impact breccia on the basin floor, indicating a significant period of time before the onset of volcanic activity in Schrödinger. The sequence of volcanic events with respect to each other has not yet been quantitatively determined.

Where's the Water?

The chemistry of sampled lunar volcanic glasses indicates that they experienced very little fractional crystallization during their ascent to the surface - they have pristine melt compositions [e.g., 16]. Volatile abundances, including OH, measured in some lunar volcanic glasses [17,18] has been the basis for modeling a water abundance of ~700 ppm in mantle, or at least the mantle source of the analyzed glasses. Incompatible trace elements abundances measured in the same glasses showed a positive correlation with OH and other volatiles [19], which is expected since water is also incompatible in a magma. Volatile enrichment would lower the melting temperature in the deep mantle source, and volatile exsolution in the lithosphere could provide a driving force for ascent of dense basaltic magmas through less dense anorthositic crust in dikes [8].

We used M^3 spectral data to create a map of the depth of the absorption at 2820 nm (Fig. 1b), which is attributed to the presence of OH within the top µm of the surface. Virtually all of Schrödinger's materials exhibit unambiguous spectral absorption features due to the presence of OH, testifying to the prevalence of volatiles in this polar region. The mare and pyroclastic units stand out as dark in Figure 2c, compared to the rest of the basin, because they have a much weaker OH absorption. Moreover, the crater and ejecta of a fresh impact into the pyroclastic deposit are even darker in the 2820 nm band depth image (Fig. 1d), indicating that the fresh pyroclastic material has an even lower OH abundance. Although we did not expect to observe the enrichment in OH from orbital data, such as measured in the lunar glasses by [17] and [18], the observation of a relative depletion in freshly exposed volcanic glass was unexpected, and is difficult to reconcile with the laboratory measurements. In the very least raises questions about the rate and efficiency of volatile loss and retention in different materials on the lunar surface.

References

[1] Garrick-Bethell & Zuber (2009) *Science,* **323**; [2] Uemoto et al. (2011) *LPSC 42,* #1722; [3] Wilhelms (1987) *USGS Prof. Paper 1348*; [4] Shoemaker et al. (1994) *Science* **266**; [5] O'Sullivan et al. *GSA Special Pub. 477* (2011); [6] Kramer et al., (2013) *Icarus* **223**; [7] Head (1976) *Rev. Geophys. Space Phys.*; [8] McGovern & Litherland (2011) *LPSC 42;* [9] McGovern et al. (2011) *AGU Fall Session*; [10] Kramer et al. (2011) *AGU Fall Session*; [11] Kramer et al., (2012) *LPSC 43,* #1734; [12] Jozwiak et al. (2012) *JGR* **117**; [13] Klimczak (2014) *Geology* **42**; 963-966; [14] Jozwiak et al. (2015) *Icarus* **248**; [15] Kramer et al. (2011) *LPSC 42,* #1545; [16] Delano (1986) *JGR* **91**; [17] Saal et al. (2008) *Nature*; [18] Hauri et al. (2011) *Science*; [19] Saal et al. (2011) *NASA Lunar Sci. Inst. Forum.*